This is the peer-reviewed, final accepted version for American Mineralogist, published by the Mineralogical Society of America.
The published version is subject to change. Cite as Authors (Year) Title. American Mineralogist, in press.
DOI: https://doi.org/10.2138/am-2022-8167. http://www.minsocam.org/

Revision 1, 7/8/2021

Letter

On the formation of Martian blueberries

D.D. Eberl[1]
[1]349 Mountain Meadows Rd., Boulder, Colorado 80302, U.S.A.

Abstract

The Martian blueberries, first discovered by NASA's Opportunity rover, are concretions likely formed in sediments from hydrothermal solutions resulting from bolide impact into groundwater or permafrost. Evidence for this conclusion comes from the shapes of particle size distributions measured from Opportunity photos by Royer et al. (2006, 2008). These distributions, which exhibit a unique negative skew and lognormal positive skews, fit theoretical and experimental shapes determined for minerals precipitated from solution at higher and lower levels of supersaturation, respectively. The authors of these particle size measurements suggested that the blueberries were formed by aggregation or vapor condensation from a large meteoritic impact cloud. This origin is unlikely because such an event would not have created both negative and positive skews that closely fit distribution shapes expected for mineral crystallization from solution.

Keywords: Martian blueberries, crystal growth, Ostwald ripening, Mars, concretions

METHODS AND DISCUSSION

The particle size distributions (PSDs) of ubiquitous, granule-sized, hematite spherules, nicknamed blueberries, discovered and photographed at Meridiani Planum by the Opportunity rover, were measured semiautomatically from Pancam images by Royer et al. (2006, 2008). These and

other authors (Burt et al. 2005; Misra et al. 2014; Burt 2021) favored an origin for these spherules by aggregation, vapor condensation or meteoritic melting from a large meteoritic impact cloud. Other investigators have suggested an origin by fluid-driven concretion formation (Chan et al. 2004; Grotzinger et al. 2005; McLennan et al. 2005), and, most recently, by the growth of mushrooms (Joseph et al. 2021). Based on the shapes of PSD data, the present contribution favors concretion formation by nucleation and growth from supersaturated solutions.

Figure 1 shows a typical Pancam photo from which blueberry sizes and PSD shapes were carefully determined. Figures 2 and 3 show PSD shapes measured from near Endurance Crater rim, and from approximately 5 km to the south near Victoria Crater rim. The sol number indicates the number of Martian days that the rover was on Mars, and therefore approximately marks the progress of the rover's traverse around and between these craters. Rover traverse maps are available at https://mars.nasa.gov/mer/mission/traverse-maps/opportunity/, and https://en.wikipedia.org/wiki/Opportunity_(rover).

The PSDs exhibit a regular change in shape, from left-skewed west and south of Endurance Crater rim (Figure 2, upper), to right-skewed north of Victoria Crater rim (Figure 3), with shapes transitional between the two end members west of Victoria Crater rim (Figure 2, lower). The different PSD shapes indicate origins by different growth mechanisms that appear to apply to the blueberries as well as to crystals in general. PSD shapes for blueberries and for crystals are nearly identical, and therefore it is reasonable to assume that the same equations (LSW and LPE, discussed below) apply.

The left-skewed PSDs from sols 110, 188 and 202 mimic the universal steady-state PSD shape expected for Ostwald ripening in solution according to LSW theory, an equation that was derived independently by Lifshitz and Slyozov (1961) and by Wagner (1961). Experiments

(Kile et al. 2000) have shown that this unique distribution shape reflects initial, very high levels of supersaturation, where abundant and extremely fine nuclei precipitate. A large contrast in specific surface areas among these particles leads to growth of the larger nuclei at the expense of dissolution of the smaller, less stable nuclei according to the Ostwald ripening mechanism. According to LSW theory, the PSD for any mineral that has undergone sufficient ripening will have the identical negatively skewed distribution when the data is plotted on reduced axes (size/mean size vs. frequency/maximum frequency), a shape that is independent from the initial, pre-ripened PSD shape, and that has a cutoff at large sizes.

The lognormal shapes recorded from blueberries at the rim of Victoria Crater indicate an initial precipitation of fewer and larger nuclei at smaller levels of supersaturation. These particles do not have a large enough contrast in specific surface areas after nucleation to drive ripening. They react at this level of supersaturation by surface-limited growth, forming a lognormal shape, as is described by the Law of Proportionate Effect (LPE; Eberl et al. 1998). Surface-limited growth means that the rate limiting step in crystal growth is the incorporation of growth units onto the crystal surface, rather than by their rate of transport to the surface. According to the LPE approach, the growth units are bits of crystal that are random in size, but that are generally comparable in size to the crystal itself.

Although particles could condense from an impact cloud according to the LPE to form lognormal PSDs, it is unlikely that this unidirectional process would simultaneously form the negative skew that fits the unique universal distribution shape expected for ripening.

The initial shapes of both types of distributions are formed during and immediately after nucleation, at the angstrom to nanometer scale. The relative shapes of these distributions then are preserved by transport-limited proportionate growth as the crystals increase in size and the

shapes of the original distributions are scaled up. Transport-limited growth means that the rate limiting step is the transport of growth units through solution to the crystal surface, rather than the rate of their incorporation onto the surface. In this case, the growth units also are random in size, but are small compared to the size of the crystal. Proportionate growth means that the shape of the distribution is multiplied by a scaling factor to find the new distribution shape after growth. Proportionate growth results in a constant variance (beta squared) for the distribution as mean size (alpha) increases (Kile et al. 2000; Eberl et al. 2002; Kile et al. 2003).

Thus, the Ostwald and the lognormal PSD shapes indicate the level of supersaturation near the time of nucleation, which was very high for the left skewed distributions near Endurance Crater and lower for the right skewed found near Victoria rim, with intermediate levels of supersaturation yielding PSD shapes transitional between the two extremes, as has been demonstrated in analogous calcite crystal growth experiments (Figure 4). The intermediate PSD shapes result from incomplete ripening of the initial precipitates.

In order to produce the solutions required to generate the various PSD shapes, one or more bolide impacts could have melted permafrost and heated groundwater to initiate hydrothermal systems in the surrounding rocks (e.g., Pirajano 2009). Groundwater then would respond to thermal gradients by reacting with the rock to form solutions having a range of supersaturations. The regular change in PSD shapes from Endurance crater to Victoria rim suggests decreasing initial solution concentrations in this direction, perhaps related to distance from a heat source, or to a change in stratigraphic depth as the rover moved up section from Endurance to Victoria craters (Squyres et al. 2006), or to different heatings from separate impacts.

In support of a hydrothermal origin, the true color of the blueberries, which appeared blue in false color images, is grey rather than hematite red, indicating the presence of specular hematite,

the higher temperature variety of the mineral. In addition, Fan et al. (2005) synthesized spherical hematite nanoparticles at elevated temperatures, and Morris et al. (2005) found 10-100 micron specular hematite spheres in hydrothermally altered Hawaiian basalt. Because hematite blueberries would be harder than steel (6 versus 4 on Mohs scale), they would be concentrated in lag deposits by the weathering and erosion of softer surrounding rock, as has been indicated by previous investigators cited above.

IMPLICATIONS

The initial discovery, made by Opportunity rover, of iron-rich Martian blueberries was exciting because it suggested that water was needed for their formation, and, therefore, water was present on Mars. Other workers contended that water was not needed, because the blueberries could have formed by aerial condensation of mineral clouds related to bolide impact. There is ample evidence for the presence of water on Mars, even without the blueberry evidence. However, the size distributions of the blueberries have a more detailed story to tell. Not only do the shapes of their PSDs indicate the presence of water, but they also indicate initial relative solution concentrations, and they may reveal relict concentration gradients in regional groundwater systems. More measurements of blueberry PSDs from existing rover photos may yield further information about hydrologic systems in this remote and exotic environment.

Acknowledgments

Thanks to Denis Royer for sending the author raw data from his 2008 paper, to Jan Środoń and Dan Kile for reviews of the initial manuscript, to Linda C. Kah and to an anonymous reviewer for their formal reviews, and to the USGS where this research was initiated.

References Cited

Burt, D.M., Knauth, L.P., and Wohletz, K.H. (2005) Origin of layered rocks, salts, and spherules at the Opportunity landing site on Mars: No flowing or standing water evident or required. Lunar and Planetary Science XXXVI, 1527.pdf.

Burt, D.M. (2021) Distinctive features of impactoclastic layered rocks on Mars. 52nd Lunar and Planetary Science Conference. LPI Contrib. No. 2548, pdf 1210.

Chan, M.A., Beitler, B., Parry, W.T., Ormö, J., and Komatsu, G. (2004) A possible terrestrial analogue for haematite concretions on Mars. Nature, 429, 731–734.

Eberl, D.D., Drits, V.A., and Środoń, J. (1998) Deducing crystal growth mechanisms for minerals from the shapes of crystal size distributions. American Journal of Science, 298, 499-533.

Eberl, D.D., Kile, D.E., and Drits, V.A. (2002) On geological interpretations of crystal size distributions: Constant vs. proportionate growth. American Mineralogist, 87,1235-1241.

Fan, H., Song, B., Liu, J., Yang, Z., and Li, Q. (2005) Thermal formation mechanism and size control of spherical hematite nanoparticles. Materials Chemistry and Physics, 89. 321-325.

Grotzinger, J.P. et al. (2005) Stratigraphy and sedimentology of a dry to wet eolian depositional system, Burns formation, Meridiani Planum, Mars. Earth and Planetary Science Letters, 240, 11 -72.

Joseph, R.G. et al. (2021) Fungi on Mars? Evidence of growth and behavior from sequential images. Advances in Microbiology, 11, 1-67.

Kile, D.E., Eberl, D.D., Hoch, A.R., and Reddy, M.M. (2000) An assessment of calcite crystal growth mechanisms base on crystal size distributions. Geochimica et Cosmochimica Acta, 64, 2937-2950.

Kile, D.E., and Eberl, D.D. (2003) On the origin of size-dependent and size-independent crystal growth: Influence of advection and diffusion. American Mineralogist, 88, 1514-1521.

Lifshitz, I.M., and Slyozov, V.V. (1961) The kinetics of precipitation from supersaturated solid solutions. Journal of Physics and Chemistry of Solids, 19, 35-50.

McLennan, S.M. et al. (2005) Provenance and diagenesis of the evaporite-bearing Burns formation, Meridiani Planum, Mars. Earth and Planetary Science Letters, 240, 95-121.

Misra, A.K., Acosta-Maeda, T.E., Scott, E.R.D., and Sharma, S.K. (2014) Possible mechanism for explaining the origin and size distribution of Martian hematite spherules. Planetary and Space Science, 92, 16-23.

Morris, R.V. et al. (2005) Hematite spherules in basaltic tephra altered under aqueous, acid-sulfate conditions on Mauna Kea volcano, Hawaii: Possible clues for the occurrence of hematite-rich spherules in the Burns formation at Meridiani Planum, Mars. Earth and Planetary Science Letters, 240, 168–178.

Pirajno, F. (2009) Hydrothermal processes associated with meteorite impacts. In: Hydrothermal Processes and Mineral Systems. Springer, Dordrecht, 1025-1096.

Royer, D., Nelson, J., and Wallace, H.C. (2006) Mars spherule size distribution from panoramic camera images. Lunar and Planetary Science Conference (No. XXXVII), Abstract #1001.

Royer, D., Burt, D.M., and Wohletz, K.H. (2008) The Mars spherule size distribution and the impact hypothesis. Lunar and Planetary Science Conference (No. XXXIX), Abstract #1013.

Squyres, S.W. et al. (2006) Overview of the Opportunity Mars exploration rover mission to Meridiani Planum: Eagle Crater to Purgatory Ripple. Journal of Geophysical Research, 111, E12S12, doi:10.1029/2006JE002771.

Wagner, C. (1961) Theorie der alterung von niederschlägen durch umlösen (Ostwald reifung). Zeitschrift fuer Elektrochimie, 65, 581-591 (in German).

List of Figure Captions

Figure 1. Pancam image of Martian blueberries (from Royer et al. 2006). The average particle diameter is 3.73 mm.

Figure 2. Changes in the shapes of particle size distributions as the rover neared Endurance Crater rim (upper) and Victoria Crater rim (lower), showing a change from the universal steady-state Ostwald-shaped reduced PSDs (upper) to transitional PSDs (lower). The original PSD data comes from Royer et al. (2008).

Figure 3. The two best examples of lognormal PSDs from Victoria Crater rim. The other four samples in this data set skew to the right, and pass the Kolmogorov-Smirnov statistical test for log normality: sol 1124 from 1 to 5%, sol 1071 from 5 to 10%, and sols 1113 and 1139 (and the two sols shown above) to the >10% level of confidence, the highest level in the tables. The original PSD data comes from Royer et al. (2008).

Figure 4. Reduced plot giving PSD results for calcite crystal nucleation and growth experiments initiated at different levels of supersaturation (omega). The largest omega (100) yields the universal steady state shape for Ostwald ripening. A smaller omega (40) yields a lognormal distribution, and an intermediate omega (69) gives a shape intermediate between the two. (From Kile et al. 2000).

This is the peer-reviewed, final accepted version for American Mineralogist, published by the Mineralogical Society of America.
The published version is subject to change. Cite as Authors (Year) Title. American Mineralogist, in press.
DOI: https://doi.org/10.2138/am-2022-8167. http://www.minsocam.org/

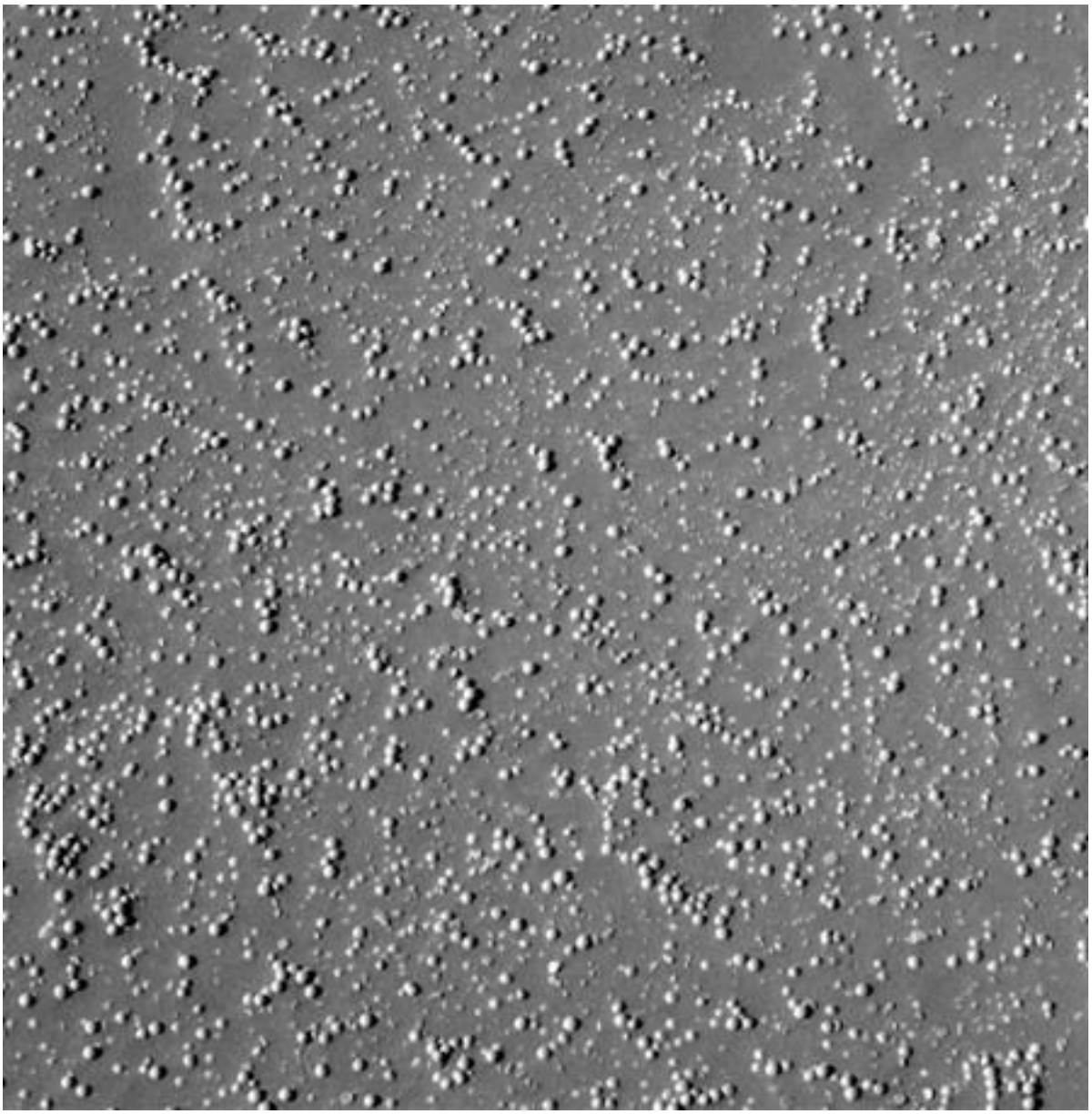

177 **Figure 1.**

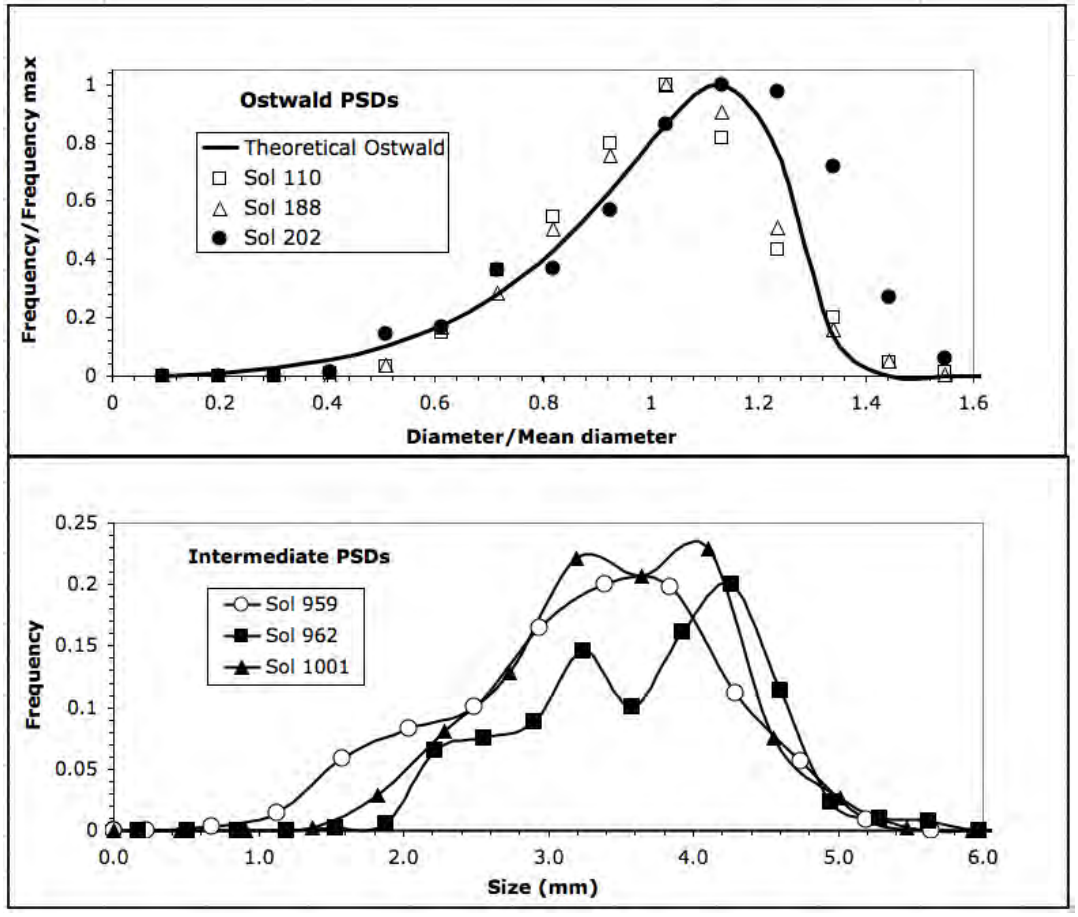

178 **Figure 2.**

This is the peer-reviewed, final accepted version for American Mineralogist, published by the Mineralogical Society of America.
The published version is subject to change. Cite as Authors (Year) Title. American Mineralogist, in press.
DOI: https://doi.org/10.2138/am-2022-8167. http://www.minsocam.org/

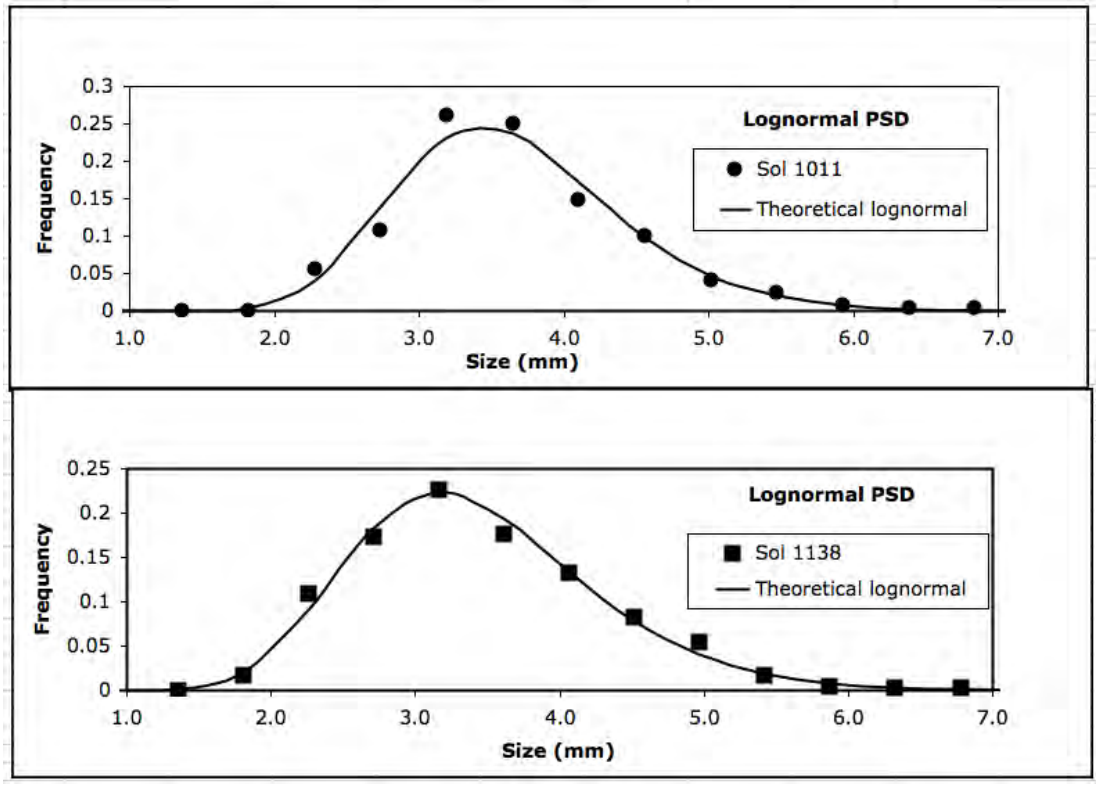

179 **Figure 3.**

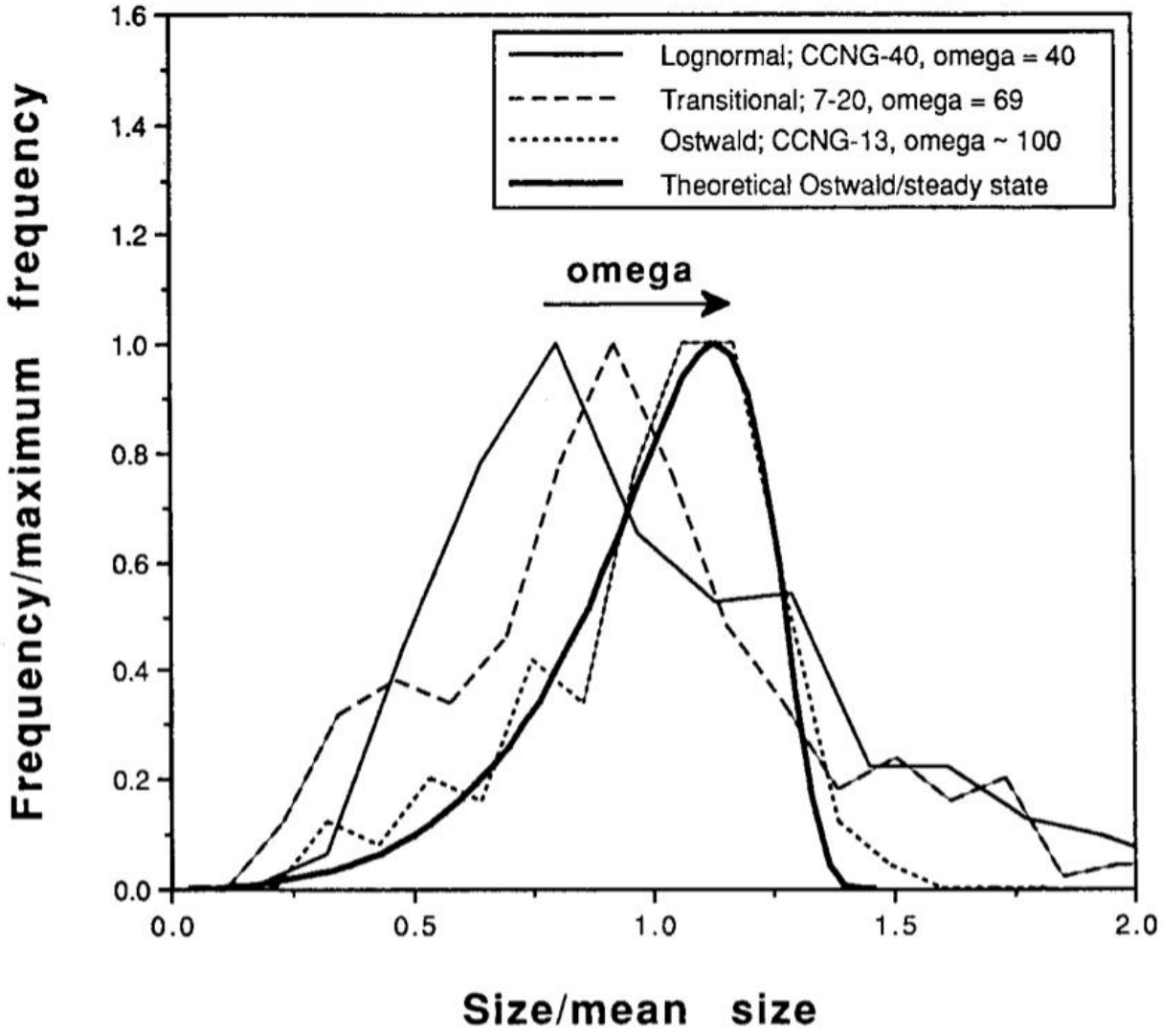

180

181